



Treball Final de Grau

Influence of the composition on the properties of $(\text{Bi}_{0.5}\text{Na}_{0.5})\text{TiO}_3$ based lead-free ceramics.

Influència de la composició en les propietats de ceràmiques lliures de plom basades en $(\text{Bi}_{0.5}\text{Na}_{0.5})\text{TiO}_3$.

Albert Royo Rodríguez

January 2016

Aquesta obra esta subjecta a la llicència de:
Reconeixement–NoComercial–SenseObraDerivada



<http://creativecommons.org/licenses/by-nc-nd/3.0/es/>

Do, or do not. There is no try.

Yoda

Dono les gràcies a la meva família per haver estat un suport fonamental a la meva vida i per no deixar-me llençar la tovallola i rendir-me quan he estat en els meus pitjors moments. També agraeixo als meus amics de Maristes per haver estat sempre quan els he necessitat i haver-me donat sempre injeccions d'ànims que m'han permès arribar fins on he arribat. No m'oblido dels meus amics i amigues de la universitat amb els qui he pogut xerrar, riure, discutir i bromejar durant la carrera però que també han estat un pilar de suport fonamental durant aquests anys. Agraeixo a la meva tutora del Treball Final de Grau, la Doctora Lourdes Mestres Vila, tots els consells que m'ha anat donant durant aquests quatre mesos i haver estat sempre disponible quan tenia dubtes o quan em trobava en un carreró sense sortida. Un especial agraïment a l'Elena Cerdeiras, que ha estat ajudant-me i ensenyant-me tot el que havia de saber i aprendre per a realitzar el treball el millor possible. Finalment, agraeixo també a la resta del grup QES de la Universitat de Barcelona, Neus i Marcos, per haver-me fet sentir un més de la família durant la meva breu, però inoblidable, estada amb vosaltres al laboratori.

REPORT

CONTENTS

1. SUMMARY	3
2. RESUM	5
3. INTRODUCTION	7
4. OBJECTIVES	9
5. THEORY FUNDAMENTALS	11
5.1 Solid state reaction	11
5.2 Perovskite structure	12
5.3 Piezoelectric and ferroelectric materials	13
5.4 Lead-free dielectric materials	15
5.5 Bismuth Sodium titanate doped with barium titanate (BNT-BT)	16
5.6 Characterization techniques	18
5.6.1 Infrared Spectroscopy (IR)	18
5.6.2 Scanning Electron Microscopy (SEM)	19
5.6.3 Energy Dispersive X-Ray Spectroscopy (EDS)	20
5.6.4 X-Ray Diffraction (XRD)	21
5.6.5 Impedance Spectroscopy (IS)	22
6. EXPERIMENTAL SECTION	26
7. CHARACTERIZATION	30
7.1 Infrared Spectroscopy (IR)	30
7.2 Scanning Electron Microscopy-Energy Dispersive X-Ray Spectroscopy (SEM/EDS)	31
7.3 X-Ray Diffraction (XRD)	35
7.4 Impedance Spectroscopy (IS)	39
8. CONCLUSIONS	42
9. REFERENCES AND NOTES	44

1. SUMMARY

Piezoelectric and ferroelectric materials are used in a wide range of applications, and lead zirconate titanate-based (PZT) ceramics are the most used piezoelectric materials. PZT shows great dielectric and functional properties. However, due to the cataloging of PZT as a hazardous material by the European Union the need for researching on lead-free ceramics with similar properties that PZT presents has increased. During last years, new materials not harmful for the environment and for human health have been studied.

Bismuth Sodium titanate (BNT) is presented as a possible candidate to replace PZT, as it shows good ferroelectric behavior with remanent polarization $38\mu\text{C}/\text{cm}^2$ and has the Curie temperature at 320°C . However, a huge issue of BNT ceramics is that BNT is hard to polarize due to the high coercive field and high conductivity caused by the loss of volatile elements as bismuth and/or Sodium so BNT usage as a piezoelectric material is limited.

In order to follow the same strategy used in the PZT, in this work the ceramic method has been used to synthesize the bismuth Sodium titanate doped with barium titanate (BNT-BT). The $(1-x)(\text{Bi}_{0.5}\text{Na}_{0.5})\text{TiO}_3-x\text{BaTiO}_3$ system has a MBP between $x=0.06-0.07$, a region where the rhombohedral and tetragonal phases coexist and wherein a relevant improvement of the functional properties of the ceramic is detected.

In this essay, the BNT-BT was synthesized using 5% and 20% excess of Sodium with the purpose of studying how that excess affects the piezoelectric properties of the BNT-BT. BNT-BT with Sodium excess was prepared by solid state reaction as it is a reproducible and scalable method as well as economic and technology viable.

The temperature used for the calcinations of the mixture of the reagents was 700°C . The resulting IR spectra of the calcined powder and the mixture of the reagents indicated the absence of carbonates and water on the calcined powder, and confirmed the formation of the perovskite structure of the BNT-BT after the treatment at 700°C .

Once the reaction was completed, and in order to densify the material, knowing that the best functional properties have a close relation with the density of the ceramics, BNT-BT ceramics were sintered at different temperatures 1200°C, 1150°C and 1100°C.

The microstructural and compositional analysis of the surface of the ceramics using the Scanning Electron Microscopy (SEM) coupled with Energy Dispersive X-Ray Spectroscopy (EDS) show that the dense ceramics present a non homogeneous chemical composition on the surface on the ceramics where two different phases, one of BNT-BT and another of Sodium Titanate, were found. Regarding grain morphology, shape changes were found with the addition of more Sodium excess.

Based on the sintering temperature and the amount of Sodium, the materials present different crystalline structures and different degrees of crystallinity as was observed using X-Ray Diffraction (XRD). The BNT-BT phases found were pseudocubic perovskite structure for ceramics with 5% Sodium excess sintered at 1150°C and 1100°C and triclinic for the 5% Sodium excess sintered at 1200°C and all the ceramics sintered with a 20% of Sodium excess. On all the studied cases it was observed the presence of a secondary phase. It was proven that this phase found on the ceramics was Sodium Titanate which can be found with a monoclinic structure when is treated at 800°C or rhombohedral structure at 900°C.

Finally, using Impedance Spectroscopy (IS), it could be observed how the sintering temperature have not influence on its behavior as a dielectric material. However, the amount of Sodium excess affects the dielectric behavior of the material.

Keywords: Piezoelectric materials, BNT-BT, solid state chemistry, lead-free, electrical properties, perovskite.

2. RESUM

Les ceràmiques basades en el titanat zirconat de plom (PZT) són els materials piezoelèctrics i ferroelèctrics més emprats i amb més aplicacions. El PZT presenta unes molt bones propietats funcionals i dielèctriques. Malgrat tot, degut a que la Unió Europea va catalogar el PZT com a material perillós degut a la seva alta toxicitat, la necessitat de trobar ceràmiques lliures de plom però amb propietats semblants al PZT es va incrementar. Durant els darrers anys, s'han investigat nous materials no nocius per al medi ambient i la salut dels éssers humans.

El titanat de bismut i sodi (BNT) es presenta com un possible candidat a substituir el PZT, donat que mostra un bon comportament ferroelèctric amb una polarització remanent de $38\mu\text{C}/\text{cm}^2$ i una temperatura de Curie de 320°C . Malgrat tot, un problema de les ceràmiques de BNT és que el BNT és difícil de polaritzar degut a l'alt camp coercitiu i l'alta conductivitat deguda a les pèrdues d'elements volàtils com el bismut i el sodi, així que la utilització de les ceràmiques basades en el BNT tenen un ús limitat.

Per tal de seguir la mateixa estratègia emprada en el PZT, en aquest treball s'ha sintetitzat el titanat de bismut i sodi dopat amb titanat de bari (BNT-BT). El sistema $(1-x)(\text{Bi}_{0.5}\text{Na}_{0.5})\text{TiO}_3$ - $x\text{BaTiO}_3$ presenta una MPB entre $x=0.06$ - 0.07 on les fases romboèdrica i tetragonal coexisteixen i, en la que es detecta una millora important de les propietats funcionals del ceràmic.

En aquest treball, el BNT-BT es va sintetitzar emprant un excés del 5% i del 20% en sodi amb l'objectiu d'estudiar com aquest excés afecta les propietats piezoelèctriques del BNT-BT. El BNT-BT amb excés de sodi es va preparar mitjançant reacció en estat sòlid ja que es un mètode molt reproducible i viable econòmicament i tecnològicament.

La temperatura emprada per a la calcinació de la mescla de reactius va ser de 700°C . Els resultats dels espectres IR de la pols calcinada i de la mescla de reactius indiquen la absència de carbonats i aigua a la pols calcinada i confirma la formació de l'estructura de perovskita del BNT-BT després del tractament a 700°C .

Un cop la reacció es va completar, i per tal de densificar el material sabent que, les millors propietats funcionals dels ceràmics guarden relació amb la seva densitat, la pols de BNT-BT amb excés de sodi es va sinteritzar a les diferents temperatures de 1200°C, 1150°C i 1100°C.

L'anàlisi microestructural i composicional de la superfície de les ceràmiques emprant Microscòpia Electrònica de Rastreg (SEM) i Espectroscòpia d'Energia Dispersada de Raigs-X (EDS) posen de manifest que les ceràmiques denses mostren una composició química no homogènia de la superfície de la ceràmica on es poden observar dues fases diferents, una de BNT-BT i una de titanat de sodi. També es van trobar canvis en la seva morfologia depenent de la quantitat d'excés de Sodi.

En funció de la temperatura de sinterització i del contingut de sodi, els materials presenten diferents estructures cristal·lines i diferent grau de cristal·linitat segons s'ha pogut determinar per Difracció de Raigs X (XRD). Les fases trobades del BNT-BT foren de perovskita amb estructura pseudocúbica per a les ceràmiques amb un 5% d'excés de sodi sinteritzades a 1150°C i 1100°C i amb estructura triclínic per la sinteritzada a 1200°C així com també per a totes les ceràmiques sinteritzades amb un excés del 20% en sodi. En tots els cassos s'ha observat la presència d'una fase secundària (<1%). Es va demostrar que aquesta fase secundària es titanat de sodi el qual es pot trobar amb estructura monoclínic quan es tracta a 800°C o romboèdrica quan es tracta a 900°C.

Finalment, mitjançant espectroscòpia d'impedàncies s'ha observat com la temperatura de sinterització no influeix en el seu comportament com a material dielèctric, però sí que ho fa l'augment de la presència de sodi.

Paraules clau: Materials piezoelèctrics, BNT-BT, química de l'estat sòlid, lliures de plom, propietats elèctriques, perovskita.

3. INTRODUCTION

Jacques and Pierre Curie first studies about piezoelectricity were published during the last years of the XIX century [1]. Those studies were focused in the production of electricity by the application of a mechanical stress on different materials. This effect is now known as “direct piezoelectric effect”.

Since the discovery of the piezoelectric effect until nowadays, studies related to this phenomenon helped the development of new materials and devices. During the World War I, under military interests, research and development for new applications and devices facilitated the development of sonar piezoelectric devices (Langevin's Transducer) [2] and the discovery of a solid solution of lead zirconate titanate with formula $\text{Pb}(\text{Zr}_x\text{Ti}_{1-x})\text{O}_3$ also called PZT [3].

PZT, was chosen as the piezoelectric reference material due to its exceptional functional properties and its great versatility and its discovery represented a big jump in the use and application of these materials [4]. In the phase diagram of PZT, for a composition of titanate and zirconate around $x=0.5$, PZT shows a phase transition that depends on the concentration and partially on the temperature, known as morphotropic phase boundary (MPB). In that composition, PZT shows a considerable improvement of the piezoelectric, dielectric and ferroelectric properties [5]. However, PZT's main disadvantage is that lead is a highly volatile toxic element [6] and, as a consequence, in 2003 the European Union opted to officially classify lead zirconate titanate based materials as hazardous substances [7] [8]. In recent years, broad research has focused on the development of lead-free alternative piezoelectric materials in substitution of lead zirconate titanate ceramics.

Bismuth Sodium titanate (BNT) was found to be an excellent lead-free material in substitution of PZT. BNT is a good ferroelectric material with a remnant polarization of $38\mu\text{C}/\text{cm}^2$ and a Curie temperature of 320°C . In addition, the dielectric properties display an anomaly wherein the low temperature phase transition at 200°C marks the transition from the ferroelectric to the antiferroelectric phase [9]. However, a huge issue of BNT ceramics is that BNT is hard to polarize due to the high coercive field and high conductivity caused by the loss of

volatile elements as bismuth and/or Sodium so BNT usage as a piezoelectric material is limited [10]. In order to improve BNT properties, barium titanate (BT) was introduced in the structure forming a BNT based solid solution (BNT-BT) [11]. Just as PZT, $(1-x)(\text{Bi}_{0.5}\text{Na}_{0.5})\text{TiO}_3-x\text{BaTiO}_3$ has a MBP between $x=0.06-0.07$, region where the rhombohedral and tetragonal phases coexist.

In this essay, the BNT-BT was synthesized using 5% and 20% excess of Sodium with the purpose of studying how that excess affects the structure, microstructure and piezoelectric properties of the BNT-BT. BNT-BT with Sodium excess was prepared and sintered by solid state reaction as it is a reproducible method as well as economically and technologically viable.

The process was studied by typical solid state chemistry characterization techniques as X-Ray Diffraction, Infrared Spectroscopy, Scanning Electron Microscopy and Energy Dispersive X-Ray Spectroscopy. The electrical properties were studied by Impedance Spectroscopy.

4. OBJECTIVES

The main objective of this essay is to study the effects of Sodium excess on $(1-x)(\text{Bi}_{0.5}\text{Na}_{0.5})\text{TiO}_3-x\text{BaTiO}_3$. This general objective is concreted in the following specific objectives.

- Synthesis and sintering of the $(1-x)(\text{Bi}_{0.5}\text{Na}_{0.5})\text{TiO}_3-x\text{BaTiO}_3$ with an excess of Sodium.
- Study of the effects of Sodium excess on the structure and microstructure with different experimental techniques:
 - a. Analyze the structure of the ceramic by X-Ray Diffraction (XRD)
 - b. Determine the morphology and chemical composition of the materials by Scanning Electron Microscopy (SEM/EDS).
 - c. The homogeneity of the samples will be investigated by Energy Dispersive X-Ray electron Spectroscopy (EDS)
- Study the electrical response of the material through Impedance Spectroscopy

5. THEORY FUNDAMENTALS

The purpose of this category is to introduce the main concepts to understand the whole essay.

5.1 SOLID STATE REACTIONS

A chemical reaction between species (atoms, ions or molecules) can take place if those species coincide in the same point of space at the same time. Because of that, high mobility of the reactants is usually required. This procedure is usual for reactions taking place in liquid or gas state. However, in solid state, the mobility of the particles is very low or almost nonexistent at room temperature. For this reason, to produce a reaction between substances in the solid state it is crucial to improve the mobility of the particles in the solid allowing the diffusion of the components to create a new substance.

The ceramic method, or solid state reaction, was the first approach to synthesize solids from solid precursors. This method is based on heating a mixture of precursors (usually carbonates or oxides) at high temperatures in order to enhance the diffusion of the substances [13]. The homogeneity of the reactant mixture and the size of the particles are factors that can affect the reaction. The smaller the size of the particles, the most surface contact between different particles so, the reaction will be easier. The size of the particles can be diminished with a manual mortar or by planetary milling. On the other hand, if the mixture is homogenous and the reactant phases are in close contact, the diffusion will take place through the grain boundaries.

As the new phase grows in the grain boundaries, the formation of product would become harder since the new phase will not allow contact between the reactants. The homogenization of the mixture of reactants, the reduction of the size of the particles and cyclic treatments of milling and calcination has been proved to solve this issue.

5.2 PEROVSKITE STRUCTURE

A lot of piezoelectric and ferroelectric materials have perovskite structure. Perovskite is the name of the mineral CaTiO_3 and has given name to a whole family of crystalline materials with general formula ABO_3 that share that same structure. Perovskite structure can accept a great variety of cations in A sites like Sodium, potassium, lead and lanthanides, and B sites can be occupied by almost any transition metal. Oxygen can be replaced by chlorine, fluorine or bromine. Perovskite oxides show electrical and magnetic properties that make them very attractive and that is the reason they have been studied extensively in order to attain new materials with improved properties.

Figure1 shows the perovskite lattice. The main structure is formed by BO_6 octahedrons linked by its vertex and the octahedral interstices are occupied by A cations with coordination 12.

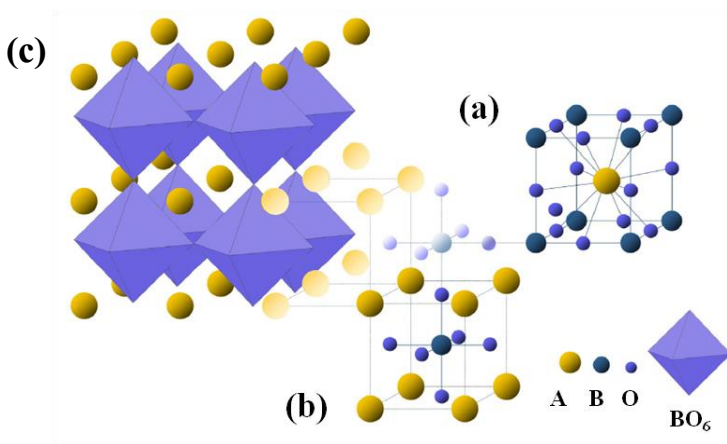


Figure 1: Different representations of perovskite structure. (a) Representation with A ions at the center of the cube. (b) Representation with B ions at the center of the cube. (c) Tridimensional representation of the union of BO_6 octahedrons.

A lot of perovskite structured compounds have structural transformations that can create little local distortions and, consequently, giving as a result the generation of low symmetry structures [14][15]. Those distortions are usually caused by atomic movement as can be seen in the **Figure2**.

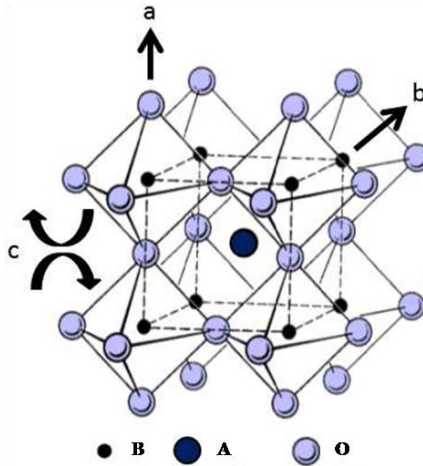


Figure 2: Atomic movement on perovskite structures. (a) Stretching of O octahedrons surrounding the B cation. (b) Movements of the B cation. (c) Spinning of BO_6 octahedrons, modifying the shape of the cavity occupied by the A cation.

The different movements, along with the creation of anionic and cationic holes, and the incorporation of different cations on A or B sites, cause variations of the perovskite structure and, consequently, modifications of the attributes of the materials.

5.3 PIEZOELECTRIC AND FERROELECTRIC MATERIALS

Piezoelectricity, also called the piezoelectric effect, is the ability of certain materials to generate an electric charge when mechanically stressed. The opposed effect, caused by the application of an electric field, is called inverse piezoelectric effect.

On piezoelectric materials, the application of a mechanical force induces dipolar moments to the system. In addition, all piezoelectric materials are also dielectric materials.

Dielectric materials are all those materials that, in normal conditions, are electrical insulators. Dielectric materials can only show up electrical conductivity when they are irradiated

with high energy radiation or high electric fields. Dielectric materials can show up piezoelectric, pyroelectric and ferroelectric properties.

On some piezoelectric materials, called pyroelectric materials, the dipoles can be created by the effect of the temperature, heating or cooling, even without an external electric field. Furthermore, some of those pyroelectrics can show spontaneous electrical polarization that can be modified by an electric field. Those materials are called ferroelectrics and, together with pyroelectric materials, are considered piezoelectric materials. Therefore, all piezoelectric materials are dielectrics.

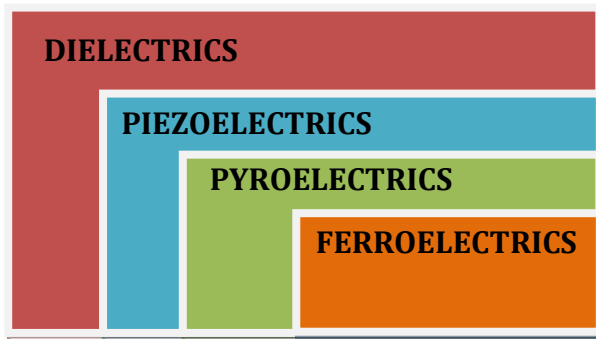


Figure 3: Classification of dielectric materials.

When an electric field is applied on a dielectric material, which dipoles are randomly oriented, the dipoles orientate themselves following the field's direction as the applied field increases. **Figure 4** represents the variation of the polarization (P) of a ferroelectric material depending on the electric field values (E).

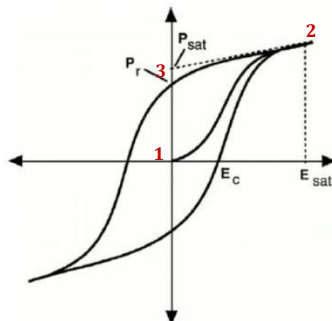


Figure 4: Hysteresis cycle of a ferroelectric material.

At the point 1 of the **Figure 4**, the polarization process begins. At 2 all the dipoles are oriented in the same direction as the electric field, that point is known as polarization saturation point (P_{sat}). When the electric field is removed ($E=0$) the material remains polarized. Point 3 of **Figure 4** indicates the remanent polarization (P_r) of the material when there is no electric field applied. Also, in order to nullify the polarization, an inverse electric field, also called coercive field (E_c), should be applied.

This typical behaviour of ferroelectric materials is usually shown at low temperatures since with increase of the temperature the material can undergo structural changes modifying its ferroelectric properties. The temperature at which a ferroelectric material loses its properties is called Curie Temperature (T_c). Over this temperature the polarization value is nullified and the ferroelectric phase changes to a paraelectric phase.

Those materials have very important applications in a lot of fields as sensors, actuators and transducers which are integrated in a wide variety of devices as much in medical instrumentation as in information processes among others.

5.4 LEAD FREE DIELECTRIC MATERIALS

One of the most used materials for sensors, actuators and piezoelectric transducers [3] is lead zirconate titanate, $\text{Pb}(\text{Zr},\text{Ti})\text{O}_3$ also known as PZT. One important characteristic of PZT is the improvement of electromechanical properties near 50% Titanium and 50% Zirconium composition because the rise of polarizability, which is caused by the existence of two equivalent energy states, a tetragonal and a rhombohedral phase [5]. This composition region is also known as morphotropic phase boundary (MPB) as can be seen in **Figure 5**.

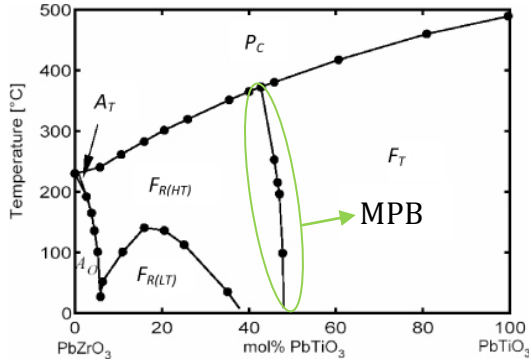


Figure 5: PZT phase diagram. P_C : Paraelectric cubic phase, $F_R(HT)$: ferroelectric rhombohedral phase at high temperature, $F_R(LT)$: ferroelectric rhombohedral phase at low temperature, A_o : anti-ferroelectric orthorhombic phase, F_t : ferroelectric tetragonal phase.

(Image extracted from B.Jaffe, W.R.Cook, and H.Jaffe. *Piezoelectric Ceramics*. Academic Press, USA (1971))

One of the drawbacks of lead based ceramics is human's health and environmental impact. Lead is a very volatile element and, during the ceramic process, it volatilizes in oxide form which is very toxic. This oxide is transmitted then to the environment where it can remain for a long time and also being accumulated on living beings. For this same reason, European laws limits lead based ceramics on electronic devices.

Due to that restriction, the research of new lead free dielectric materials with similar properties of PZT has been boosted in the last years. Some of the most prominent new materials are bismuth Sodium titanate [16], barium titanate [17] and Sodium and potassium niobates [18][19].

5.5 BISMUTH SODIUM TITANATE DOPED WITH BARIUM TITANATE (BNT-BT)

Bismuth Sodium titanate (BNT) is an excellent lead free material candidate in substitution of PZT. BNT is a good ferroelectric material with an elevated remaining polarization and a Curie temperature of 320°C. The biggest drawback of BNT ceramics is that they are very hard to polarize because BNT has a high coercive field and high conductivity caused by the loss of

volatile elements (Sodium and/or Bismuth). This fact restricts BNT ceramics use as piezoelectric materials.

For that reason and in order to synthesize a BNT-based materials with MPB, barium titanate (BT) is introduced into the BNT structure. The $(1-x)(\text{Bi}_{0.5}\text{Na}_{0.5})\text{TiO}_3$ - $x\text{BaTiO}_3$ system, known as BNT-BT, shows a MPB between $x=0.06$ - 0.07 , in that region rhombohedral and tetragonal phases can coexist.

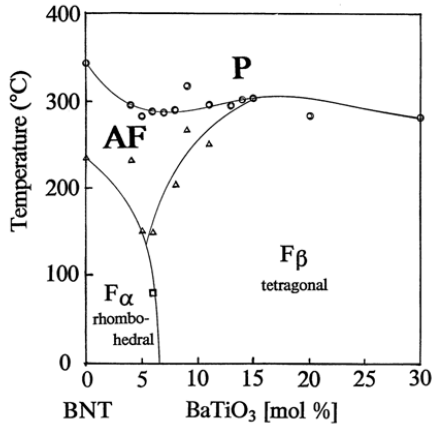


Figure 6: Phase diagram of $(1-x)(\text{Bi}_{0.5}\text{Na}_{0.5})\text{TiO}_3$ - $x\text{BaTiO}_3$ (BNT-BT) showing the Antiferroelectric (AF) region, the Paraelectric (P) one and both Ferroelectric compositions (F_α , F_β).

(Image extracted from Takenata T., Maruyama K., Sakata K. *(Bi_{0.5}Na_{0.5})TiO₃-BaTiO₃ System for Lead-Free Piezoelectric Ceramics. Japanese Journal of Applied Physics, 30(9B):2236-2239, 1991)*

At the MPB composition, BNT-BT has the best functional properties and, in reference to the electrical properties, there is dependence between temperature, the dielectric constant (ϵ_r) and also the dielectric losses ($\tan \delta$).

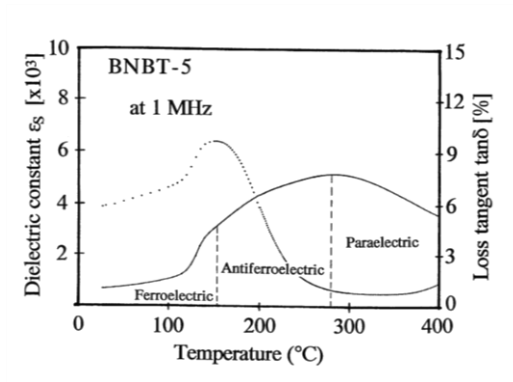


Figure 7: Dependence of the dielectric constant (ϵ_r) and the losses ($\tan \delta$) with the temperature of BNT-BT at the MPB.

(Image extracted from Takenata T., Maruyama K., Sakata K. *(Bi_{0.5}Na_{0.5})TiO₃-BaTiO₃ System for Lead-Free Piezoelectric Ceramics. Japanese Journal of Applied Physics, 30(9B):2236-2239, 1991)*

5.6 CHARACTERIZATION TECHNIQUES

5.6.1. Infrared Spectroscopy (IR)

Infrared (IR) Spectroscopy is a useful tool to obtain information about the material properties studying the vibration frequencies of the bonds of the atoms present in the compounds. IR spectrometry studies the interaction between the matter and IR radiation. The resultant spectrum is generated from the absorption of the photons that have energy corresponding to an IR region generating a transition between vibrational levels. The absorbed energy at each wavelength that can change across the time can be registered. In addition, using the Fourier Transformation all the wavelengths can be measured at the same time.

The IR study was made with a *Thermo Nicolet Avatar 330 FT-IR* using frequencies between 400 and 4000 cm^{-1} . For that process, pellets of the sample were made solved with KBr.

5.6.2. Scanning Electron Microscopy (SEM)

The interaction of electrons with matter is a complex subject of study in which many processes like absorption, emissions and reflections are involved. Some of these processes are summarized in **Figure 8**. The amount of phenomena indicates that a lot of information can be obtained by irradiating a sample with electrons. That is the reason why many characterization techniques are based in electron-solid matter interactions. Electronic microscopy is one of those techniques.

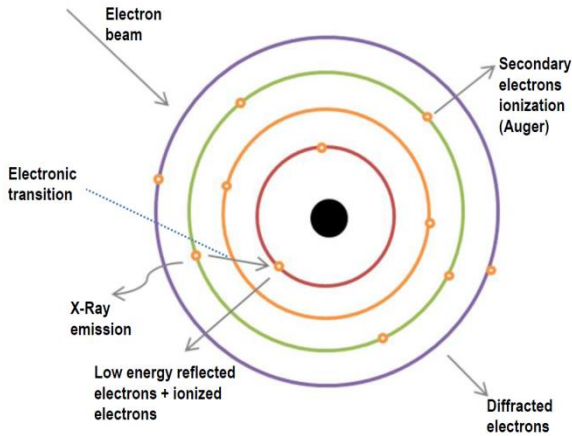


Figure 8: Electronic processes that can happen when an electron beam interacts with a sample.

The electrons used for microscopy are usually emitted by a tungsten filament or a LaB_6 crystal, with an accelerating voltage between 50 and 100kV. The most powerful High-Resolution Electron microscopies can achieve until 2\AA of resolution.

There are two main techniques within Electron Microscopy, Transmission Electron Microscopy (TEM) and Scanning Electron Microscopy (SEM).

TEM detects the electrons that pass through the sample without changing their energy. The intensity of the beam in every point of the sample gives information about the thickness and density of that point. This technique has better resolution than SEM but it needs a special pre-treatment to make the sample thin enough for this method to work.

SEM, the technique used during this characterization, the beam of electrons is focused in a small spot (50 to 100Å in diameter). Two different kinds of electrons are detected: Backscattered Electrons (BSE) and Secondary Electrons (SE). BSE are electrons scattered after an elastic collision with the atoms of the surface of the material. The scattering depends on the atomic weight of the atoms the electrons collide with: heavy atoms scatter the electrons with more strength than light atoms, for that, the contrast of the image can be related to the atoms that are present in the focused zone. Unfortunately, since these electrons are scattered by atoms that are quite deep in the solid, a three-dimensional image of the solid surface cannot be obtained. Secondary electrons are emitted by the sample when it interacts with an electron beam. These electrons are emitted in all directions by atoms that can be at 0.5 micrometers from the surface. Since the detected electrons have low energy, they are easily deviated from its trajectory and, as a result, a three dimensional image of the material can be obtained. Information about the surface's morphology and even the shape and size of single particles can be extracted from this three dimensional image. Although SEM has, in general, less resolution than TEM, it needs no special pre-treatment of the sample.

In order to perform a SEM study, the sample must have a conductive surface. For this reason the samples used for this paper were covered by a thin layer of graphite. The study of the surface of the samples was made with a *JEOL JS-6510* microscope coupled with an EDS analyzer (see below) present in the CCiTUB.

5.6.3. Energy dispersive X-Ray Spectroscopy (EDS)

The interaction of electrons with a solid gives another interesting phenomenon: when a high energy electron beam interacts with the sample, the atoms of the solid can be ionized emitting electrons from the valence shell and even inner core-shells. In order to relax the system, an electron of the valence shell decays to an inner shell emitting X-Ray radiation of a precise wavelength (corresponding to the energy gap between both shells) and characteristic of every element. On account of this, scanning those emitted X-Rays it is possible to determine the elements that are presents on the sample.

EDS is especially useful when coupled with an electronic microscope since it is possible to focus in the small portion of the observed sample to determine its morphology and at the same time analyze its composition.

For the EDS analysis, a *Stereoscan 260 EDS analyser* accessory coupled to CcITUB's SEM was used.

5.6.4. X-Ray Diffraction (XRD)

The term *diffraction* includes different processes that happen when a wave encounters an obstacle or slit with a characteristic length in the range of the wave's own wavelength.

X-Ray Diffraction is based on the scattering of an X-Ray beam colliding over the successive atomic planes of a crystal. For this reason it is mandatory that the photons have a wavelength of the same order but a bit lower than the crystalline lattice spacing. Atoms are ordered periodically on crystals, for this reason it can be expected the diffraction phenomenon to happen if a beam with a wavelength of 0.1-0.2 nm collides over the atoms. X radiation was the chosen for crystalline structure determination because it presents a wavelength of that same order. When the X-Ray beam passes through a sample it is diffracted by the different planes in many directions. Due to some interference phenomena, not every diffracted beam gets to the detector. Only the beams undergoing constructive interferences have enough intensity to be measured. Those constructive interferences of the diffracted beams give a pattern of maximums and minimums called diffraction pattern. The condition for the beams to have constructive interferences is given by Bragg's Law and its equation.

$$\text{Equation 1: } 2d\sin\theta = n\lambda$$

Bragg's Law considers that a crystal has multiple planes acting as a semi-transparent mirror and some of the X-Ray beams are reflected by the plane with an angle that equals to the incident angle as is shown in the **Figure 9**. The distance between the different crystalline lattice defining planes determinate Bragg's angle value. Because of that, the diffraction pattern gives unequivocal information of the crystalline structure.

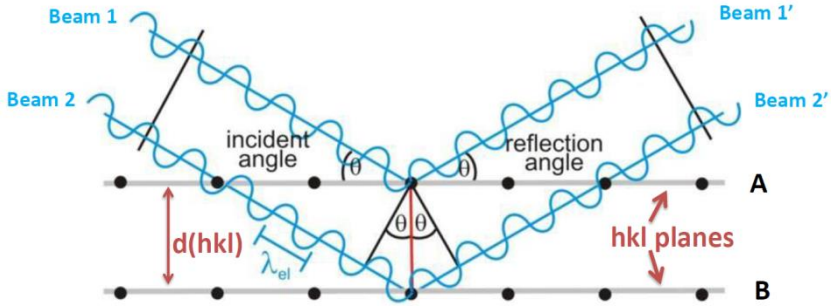


Figure 9: Representation of Bragg's Law.

The crystalline lattice is based on parallel planes (hkl) separated by a $d(hkl)$ distance. On **Figure 9** it can be observed how the first beam incidences over an atom on the A plane and is reflected with an θ angle that equals the incident angle. The second beam keeps moving on until it collides with an atom at the same position that the one before but in the next equivalent plane, in that case B plane, and it is also reflected with a θ angle that equals the incident angle. This second beam has to go through an extra (xyz) distance in comparison to the first beam. This difference with Beam 1 has to be a whole number (n), multiple of the wavelength (λ) in order to be at phase with the first reflected beam (Beam 1'). When the beams are at phase, Bragg's Law is fulfilled, meaning that the interferences are constructive and can be detected by the detector.

XRD studies were carried out with a *PANalyticalX'Pert PRO MDP Alpha1* diffractometer, with a Ge(111) monochromator. The radiation used was the $K\alpha$ line of Cu at 40kV and 30mA, and the diffraction pattern was registered for 2θ angles from 10° to 80° , with a scanning speed of $1^\circ/\text{min}$. The diffraction patterns were studied with the X'Pert HighScore50 software. The samples were compared with *Powder Diffraction File (PDF)* patterns of the *International Centre for Diffraction Data (ICDD)* database.

5.6.5. Impedance Spectroscopy (IS)

Impedance Spectroscopy is an excellent characterization technique to study the electric response of dielectric materials because it allows the separation of the different contributions to the total polarizability of the material, and therefore to the dielectric constant.

This technique is based in the application of an alternative current (AC) to a pellet of the material that is going to be studied located between two electrodes. Usually, both sides of the pellet are covered by a thin layer of gold, making both sides to work as the electrodes. This system is to be seen as a circuit such as the one seen in **Figure 10**.

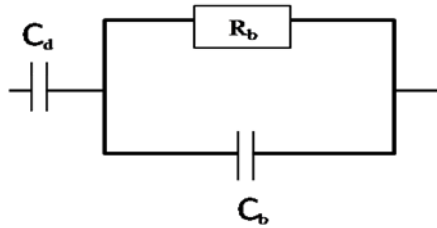


Figure 10: Equivalent circuit for a dielectric material. R_b represents the resistance the material offers to the current (high if a dielectric). The two capacitors C_d and C_b represent the capacitance of the electrodes and that of the bulk ceramic respectively.

Therefore, it is possible to relate the dielectric constant with the capacitance of this circuit:

$$\text{Equation 2: } C = \frac{\varepsilon_r \cdot A}{d}$$

Where ε_r is the relative permittivity of the material, A is the area of the sheets of the capacitor and d the distance between both sheets.

Since this is an AC system, the capacitance is a complex value with two contributions.

$$\text{Equation 3: } \varepsilon_r^* = \varepsilon_r' - j\varepsilon_r''$$

The real part (ε_r') of (Equation 3) represents the dielectric constant value while the imaginary part (ε_r'') represents the dielectric losses in form of heat.

As any imaginary number, the complex permittivity can be represented in polar coordinates as shown in **Figure 11**. In this case, the phase gap angle (δ) between Voltage and Intensity is the angle of the vector that represents the permittivity. As the frequency increases, δ changes from 90° to a minimum value (depending on the material), reducing the dielectric constant and increasing the dielectric losses.

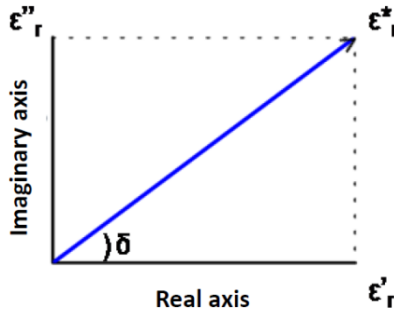


Figure 11: Representation of complex permittivity in polar coordinates.

For this study, the intensity passing through the sample for known voltage and frequency will be measured, and the impedance Z^* (i.e. the opposition that the material offers to the pass of current through it) of the system will be found. Those values can be related with **Equation 4**.

$$\text{Equation 4: } Z^* = \frac{V}{I}$$

The imaginary value of the impedance can be related with the complex value of permittivity as it is expressed in **Equation 5**.

$$\text{Equation 5: } \varepsilon_r = \frac{1}{Z^* \cdot f \cdot C_0}$$

And the two components of the complex permittivity are then separated knowing the phase lag between V and I , which is related with the AC frequency.

This analysis allows the obtaining of quantitative information about the conductance, dielectric permittivity and the dynamic properties of the interfacies. ε_r values of ferroelectric materials are influenced by the sample porosity, possible secondary phases, heterogeneity, defects, grain size, etc. On Impedance Spectroscopy currents with low frequency are used so it is a not invasive technique, which means the material electrochemical properties result unaffected after the measures.

The measures were carried out with an impedance analyzer *HP 4192A* available at the QES group of the *Universitat de Barcelona*. For the study of the electric properties, the samples

(BNT-BT pellets) were covered in gold by cathodic deposition. For every sample, capacitance and dielectric losses were measured scanning temperatures between 30 and 500°C and frequencies between 0.1 and 10000kHz.

6. EXPERIMENTAL SECTION

Two different composition of BNT-BT with general formula $0.94(\text{Bi}_{0.5}\text{Na}_{0.5})\text{TiO}_3\text{-}0.06\text{BaTiO}_3$ have been prepared, one with a 5% of Sodium excess and another one with a 20% of Sodium excess. The raw materials used for this synthesis were Bi_2O_3 , TiO_2 , Na_2CO_3 and BaCO_3 .

	Commercial reference	Purity [%]	Molecular weigh [g/mol]	Security
TiO_2	SIGMA ALDRICH	≥ 99	79.87	R10 S2, S24/25
Bi_2O_3	PROBUS	≥ 99.5	406	R36/37/38 S26/36 H315/319/335
Na_2CO_3	SIGMA ALDRICH	≥ 99.5	105.99	R36 S2/22/26/46
BaCO_3	SIGMA ALDRICH	≥ 99	197.34	R20/22 S2/28

Table 1: Raw materials used for BNT-BT synthesis.

The synthesis of both compounds were performed through a solid state synthesis process called ceramic method, that consists in heating a mixture of reactants to high temperatures in order to attain the desired product thanks to the diffusion of the atoms in the crystalline lattice.

First of all, both oxides were treated in a muffle furnace during 8 hours for total dehydration and prevent the presence of carbonates. Bi_2O_3 was treated at 500°C while TiO_2 was treated at 900°C . At the same time, Sodium and barium carbonates were heated at 200°C for 24 hours to remove any traces of water. After that, the reactants were weighted and mixed. The accuracy of the weighting process of the reactants is of critical importance since, in solid state reactions like this, the weight of the reactants will lead to the exact stoichiometry of the final product (BNT-BT). For this reason, the mixture of the reactants was executed with a precision of $\pm 0.1\text{mg}$ for every one of them.

After that, the mixture of reactants was introduced in a zirconia vessel (suitable for the planetary ball mill) using ethanol and also 1/3 of the vessel was filled by 1nm diameter zirconia

balls. The planetary ball milling process was performed to insure the mix was the most homogeneous as possible and to reduce the size of the particles. The process was done with an already optimized program for that synthesis involving 300rpm for 2 hours with a stop every 20 minutes (to cold down) and resuming but with reverse spinning. That program was repeated 3 times.

When the milling process ended, the mixture was separated from the zirconia balls using a strainer and some more ethanol. Then it was introduced in a baker for the dispersion process. The process was implemented using a disperser working at 11,000rpm for 15 minutes. A disperser is used to rapidly break lumps or agglomerates of powdery material and uniformly distributing in a liquid. Following that, the mix was heated to evaporate the ethanol and then, it was left 12 hours at 100°C to make sure its total evaporation. The resulting powder was passed through a 0.09mm mesh width sieve with the aid of a brush and placed inside an alumina crucible. This process was made to clean the powder of possible contamination (as balls or dust) and to make sure that all the powder particles had the same size.

The next stage was the thermal treatment of the mixture to obtain BNT-BT. As **Figure 12** shows, the powder was heated in a muffle furnace at 700°C for 2 hours and the treated powder was obtained. A portion of this powder was saved for later analysis and the rest milled again with the planetary ball mill, separated from the zirconia balls, dispersed at 11,000rpm this time adding 10 drops of PARALOID-67 (Rohm and Haas), a binder substance added to prevent the pellets from cracking when applied high pressures. After that, the ethanol was evaporated and the powder was passed through the 0.09mm mesh width sieve.

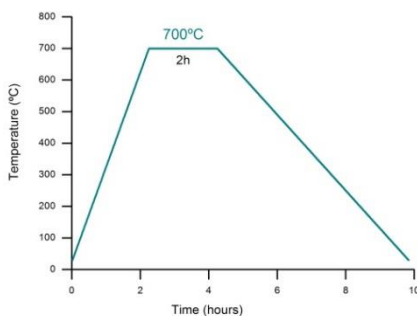


Figure 12: Thermal treatment of the mixture of reactants at 700°C versus the time.

Once the calcined powder was ready, the material had to be densified. This process was done by pressing the powder with a uniaxial press applying a pressure of 200MPa forming pellets and applying them a sintering process. Sintering is the process of compacting and forming a solid mass of material by without melting it to the point of liquefaction. In order to study the effects of the temperature of the sintering process, three sets of pellets were made. The temperatures studied were 1100°C, 1150°C and 1200°C. For each temperature 3 pellets were made, one made with 0.4g of BNT-BT powder to be studied by X-Ray Diffraction (XRD), one made using 0.2g of the powder for Scanning Electron Microscope (SEM) and another one of 0.2g for Impedance Spectrometry (IS). A total of 9 pellets were made for each BNT-BT composition. The heat treatment scheme is shown in the **Figure 13**. Each treatment consists of five ramps. The first one rises at 2°C/min till 700°C. The second one remains still at 700°C for two hours. This stop was carried out to insure the total vaporization of the binder substance. Then, the third one rises at 0.5°C/min rate till the desired sintering temperature and it stays at that temperature for two hours (4th ramp). The last step is turning back to room temperature at a 2°C/min rate.

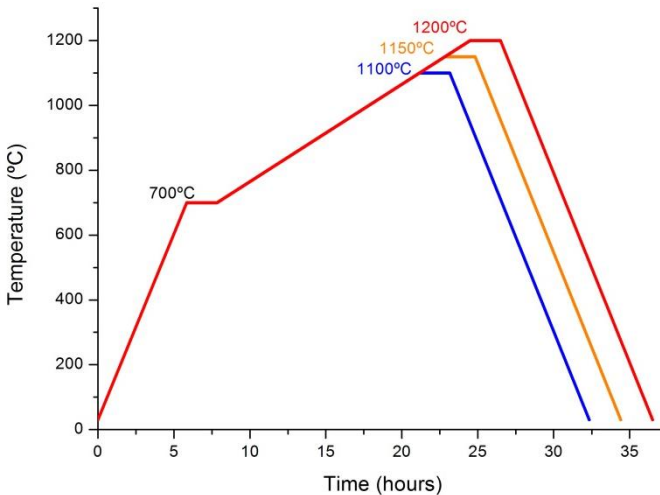


Figure 13: Thermal treatment of the sintering process of the pellets at 1200°C, 1150°C and 1100°C versus the time.

Once the treatment finished, the 0.4g pellet was crumbled to powder for the XRD analysis using an agate mortar. The other two pellets were used for SEM-EDS and IS. The one used for impedance spectrometry (IS) was the one with higher density. The density of the pellets was calculated using the Archimedes Method and its equation (**Equation 6**):

$$\text{Equation 6: } \rho = \frac{A}{A-B} \rho_0$$

Where A is the weight of the dry pellet, B is the weight of the pellet immersed in water, and ρ_0 the density of water at the weighting temperature. The experimental densities (ρ_{exp}) were the following for 5% Sodium excess (**Table1**) and 20% Sodium excess (**Table 2**).

Synt.T (°C)	A [g]	B [g]	ρ_0 [g/cm ³]	ρ_{exp} [g/cm ³]
1200	0.1780	0.1464	0.9978	5.6279
1200	0.2039	0.1657	0.9978	5.5387
1150	0.1721	0.1409	0.9978	5.2393
1150	0.1770	0.1449	0.9978	5.6291
1100	0.1490	0.1227	0.9976	5.6518
1100	0.1760	0.1439	0.9976	5.4697

Table 2: Measurement of the experimental density of 5%Na excess pellets

Synt.T (°C)	A [g]	B [g]	ρ_0 [g/cm ³]	ρ_{exp} [g/cm ³]
1200	0.1652	0.1330	0.9978	5.1191
1200	0.1644	0.1326	0.9978	5.1584
1150	0.1638	0.1389	0.9976	5.2590
1150	0.1710	0.1389	0.9976	5.3143
1100	0.1752	0.1402	0.9976	5.2358
1100	0.1698	0.1378	0.9976	5.2935

Table 3: Measurement of the experimental density of 20%Na excess pellets

As can be seen, the most the Sodium excess the pellets have, the less relative density.

The pellets chosen for SEM-EDS analysis were covered by carbon powder at the CCiTUB to increase the conductivity, which is required for the SEM-EDS process.

The pellet used for IS was covered first with a thin film of gold through a sputtering physical vapor deposition (PVD). PVD uses physical process (such as heating or sputtering) to produce a vapor of a material which is then deposited on the object that requires coating. Once the borders of the pellet have been sanded down (to prevent conductivity between both faces), and a voltage is applied to the system, both sides of the pellet act as electrodes the pellet work as electrodes and the pellet works a capacitor. Then, the electrical properties of the material can be studied.

7. CHARACTERIZATION

7.1 INFRA-RED SPECTROSCOPY (IR)

The mixture of reactants and the 5% Sodium excess BNT-BT powder treated at 700°C were studied by IR in order to confirm if the treatment was successful or if the treatment should be optimized.

The IR spectra of the mixture of the reagents show 3 important absorption bands. The band group at $\sim 850\text{cm}^{-1}$ can be assigned to the outer plane deformation of the CO_3^{2-} group (ν_3). Also, at $\sim 500\text{cm}^{-1}$ and between $630\text{-}680\text{cm}^{-1}$ the characteristic vibration peaks of Ti-O bounds can be found. The intense band at 1425cm^{-1} corresponds to the stretching of asymmetric C-O bounds of the carbonate anions and the wide band at $\sim 3300\text{cm}^{-1}$ is characteristic of the vibration of H-O bounds indicating the presence of hydroxyl groups.

On the IR spectra of the calcined powder at 700°C it can be seen how the absorption bands at 1425cm^{-1} and $\sim 3300\text{cm}^{-1}$ are not found and there is a band at $\sim 650\text{cm}^{-1}$ which matches to the vibration bands of perovskite TiO_6 octahedrons. This indicates the absence of carbonates and water while confirms the formation of the perovskite structure of the BNT-BT after the treatment at 700°C. [20,21]

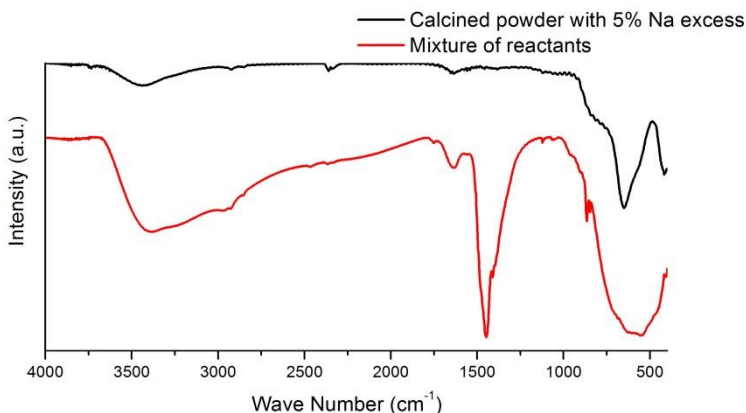


Figure 14: FT-IR spectra for the mixture of reagents and the first treatment of the mixture at 700°C.

With these results, the treatment at 700°C for 2 hours was proven to be effective so an optimization process was not needed in order to eliminate carbonates and hydroxyls.

7.2 SCANNING ELECTRON MICROSCOPY - ENERGY DISPERSIVE X-RAY SPECTROSCOPY (SEM/EDS)

The BNT-BT pellets and powder prepared were covered by a thin film of Carbon through a sputtering PVD as the Scanning Electron Microscopy requires the surface of the sample to be conductive.

The microstructure of BNT-BT ceramics with Sodium excess sintered at different temperatures was studied by Scanning Electron Microscopy (SEM) coupled with an Energy Dispersive X-Ray Spectrometer (EDS) analyzer so a visual study of the sample can be done at the same time as the composition of determined areas of the surface are studied.

This study was carried out to establish the effects of the excess of Sodium on the morphology of the BNT-BT and to estimate if the excess contributed to reach the theoretical composition of the $(1-x)(\text{Bi}_{0.5}\text{Na}_{0.5})\text{TiO}_3-x\text{BaTiO}_3$.

Relation	Theor.	+0% Na	+5% Na	+20%Na
Bi/Ti	0.47	0.48	0.47	0.48
Na/Ti	0.47	0.27	0.29	0.35
Na/Bi	1	0.58	0.61	0.73
Ba/Ti	0.06	0.06	0.06	0.06

Table 4: EDS results showing the theoretical composition of BNT-BT compounds and the results of the BNT-BT powders with 0%, 5% and 20% Sodium excess calcined at 700°C.

The results shown at **Table 4** prove that an excess of 5% Sodium is not enough to make up for the Sodium loss caused by volatilization during the calcination process. However, a 20% of Sodium excess increased the amount of Sodium in the resulting powder so, it can be conclude that a greater excess of Sodium could be used to compensate for its volatilization at that temperature.

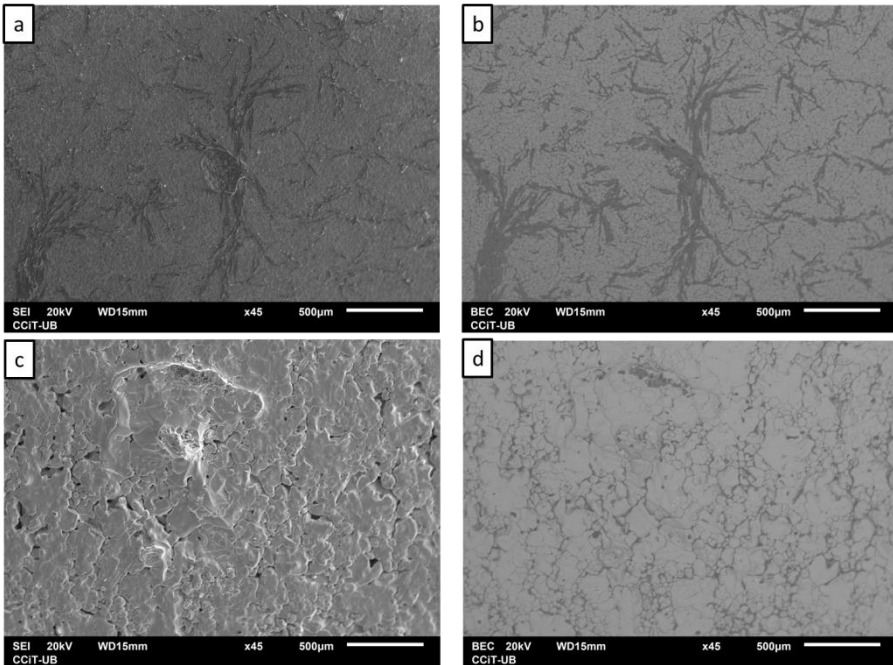


Figure 15: 45X Secondary and back scattered electrons micrographs of BNT-BT pellets sintered at 1150°C. **a)** and **b)** of a BNT-BT pellet with 5% Sodium excess. **c)** and **d)** of a BNT-BT pellet with 20% Sodium excess.

As can be seen in the **Figure 15**, the excess of Sodium affects greatly to the morphology of the surface of the pellet. The 5% Sodium excess pellet shows a homogeneous formation of grains on the whole surface while the formation of BNT-BT grains on the surface of the pellet with 20% Sodium excess is much less regular. The micrographs also show a dark area at the surface of the 5% excess pellet while it is much harder to found it on the surface of the 20% excess pellet.

An exhaustive study of the pellet allowed the study of the size and form of the grains and also, with the help of the coupled EDS the composition of both phases could be determined.

As can be seen at the **Figure 16** the microstructure of both pellets of different composition is affected by the amount of Sodium excess added. The most Sodium was added the less regular was the formation of the grains. The same happened with the pellets sintered at 1200°C and 1100°C.

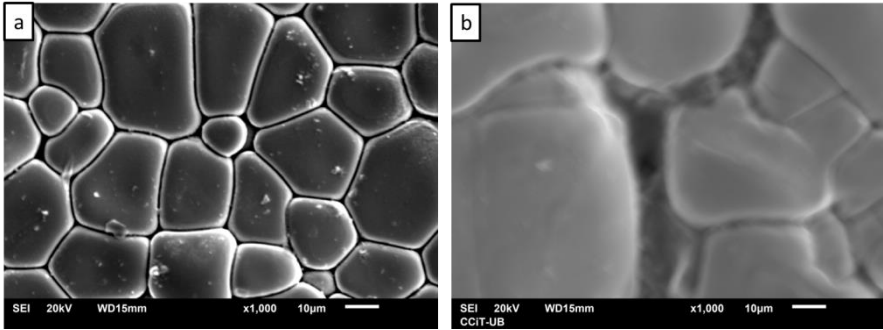


Figure 16: 1000X SEM Micrographs of BNT-BT pellets sintered at 1150°C. **a)** Corresponds to 5% Sodium excess pellet and **b)** to 20% Sodium excess

After the SEM analysis of the pellets, using the coupled EDS, a study of the composition of the pellets could be performed in specific places of the pellet allowing the study of the BNT-BT grain composition and the dark phase independently. The next tables show the results of the EDS study for the different observed phases.

Relations	Theor.	+0%Na 1200°C	+5%Na 1200°C	+5%Na 1150°C	+5%Na 1100°C	+20%Na 1200°C	+20%Na 1150°C	+20%Na 1100°C
Bi/Ti	0.47	0.50	0.49	0.47	0.5	0.49	0.49	0.5
Na/Ti	0.47	0.33	0.31	0.32	0.34	0.3	0.37	0.33
Na/Bi	1	0.67	0.64	0.67	0.67	0.60	0.74	0.66
Ba/Ti	0.06	0.06	0.06	0.06	0.08	0.06	0.06	0.06

Table 5 EDS results of the BNT-BT phase for different Sodium excess and sintering temperatures.

The results of the EDS study of the BNT-BT phase of the pellets indicates that both Sodium excesses were not helpful to increase the amount of Sodium of the sintered BNT-BT ceramic to reach the stoichiometric composition.

Atomic %	+5%Na 1200°C	+5%Na 1150°C	+5%Na 1100°C	+20%Na 1200°C	+20%Na 1150°C	+20%Na 1100°C
Na	12.42	11.29	10.82	12.90	19.89	13.62
Ti	27.12	27.44	27.92	26.88	23.39	26.53
O	60.46	60.94	61.25	60.22	56.72	59.86

Table 6: EDS results of the dark area for different Sodium excess and sintering temperatures.

The results of the EDS study of the dark area of the pellets indicate that the dark area is rich on Sodium, Titanium and Oxygen and also it lacks Bismuth and Barium.

7.3 X-RAY DIFFRACTION (XRD)

The powder calcined at 700°C was analyzed using XRD to insure the lack of impurities and assure the process was optimum. The X-Ray Diffraction pattern of the powder was obtained and, by comparison with the Powder Diffraction File (PDF) patterns of the International Centre for Diffraction Data (ICDD) database, a BNT-BT phase with perovskite structure was found as can be seen in the **Figure 17**.

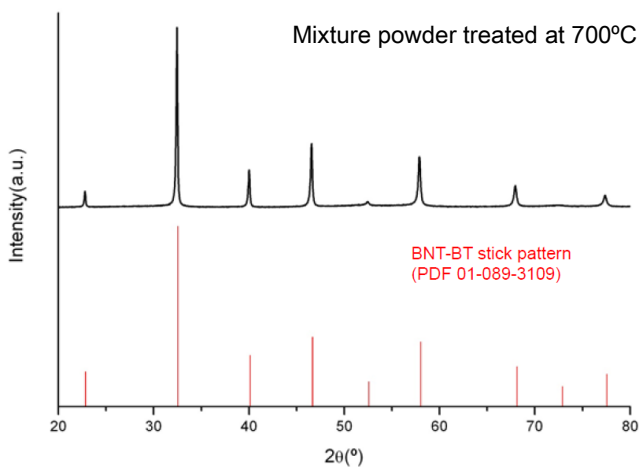


Figure 17: Comparison between XRD patterns of the powder treated at 700°C and the ICDD BNT-BT (PDF 01-089-3109) pattern.

The BNT-BT pattern shows the common pattern of a perovskite structure. The XRD results of the powder results are coherent with the BNT-BT pattern, confirming the method is optimized and the perovskite structure has been obtained. After the corroboration of the results the sintering process of the pellets began.

Figure 18 shows the results of the XRD of the BNT-BT pellets sintered with a 5% Sodium excess at different temperatures. The peaks are coherent with the BNT-BT stick pattern used and have almost the same intensity. In order to determine what kind of crystalline structure the perovskite had, an exhaustive study on the peaks at 40° and 46° was made. The study shows that, at 1200°C , there's an split of the peak at 40° which means the sintering process at 1200°C with a 5% excess of Sodium leads to a triclinic structure while at 1150° and 1100°C there are no splits, meaning the perovskite has a pseudo-cubic structure. Looking the peak at 46° a little maximum at the base of the peak can be observed (more prominent at 1200°C). That split could not be indexed as pseudo-cubic or triclinic perovskite phase so it was a secondary phase. Furthermore, a visual analysis of the back scattered electrons (BSE) micrographs indicated the presence of another phase with high Sodium, Titanium and Oxygen content. By comparing the diagram of the powder with the 40 possible Na-Ti-O compounds found on the ICDD database, focusing on the peaks representing 100% of intensity of the possible compounds, it was proven that this phase found on the BNT-BT pellets was Na_2TiO_3 which can be found with a monoclinic structure when is treated at 800°C or rhombohedral structure at 900°C so that was the reason it was not found when the powder was treated at 700°C .

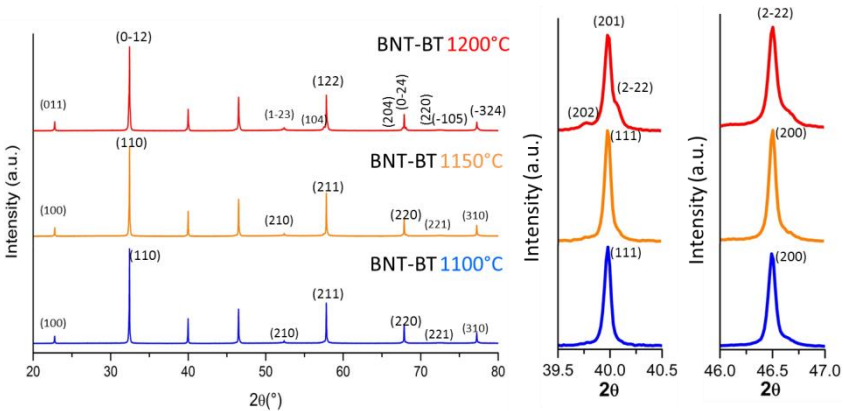


Figure 18: Comparison between XRD patterns of the BNT-BT pellets with 5% excess of Sodium sintered at 1200°C , 1150°C and 1100°C and an enlargement of the XRD around 40° and 46° .

Figure 19 shows the results of the XRD BNT-BT pellets sintered using a 20% of Sodium excess at different temperatures. At 1200°C, 1150°C and 1100°C the BNT-BT with a 20% Sodium excess can be indexed as a triclinic perovskite structure. However, at this percent of Sodium excess, the peaks are less intense than they were at the 5% Sodium excess diffractograms.

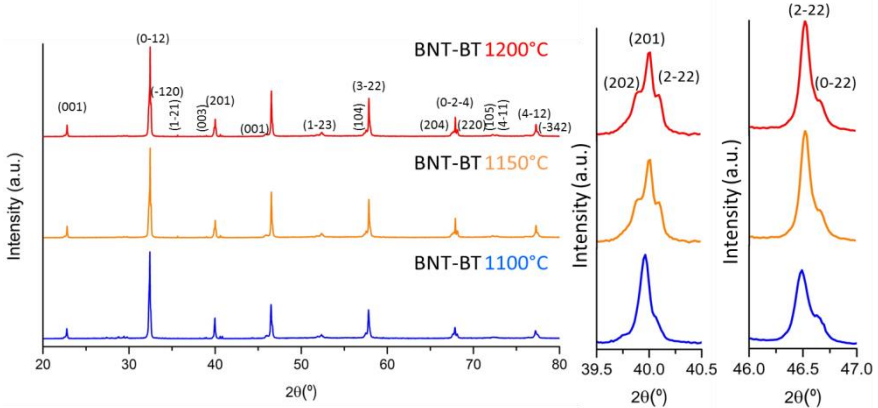


Figure 19: Comparison between XRD patterns of the BNT-BT pellets with 20% excess of Sodium sintered at 1200°C, 1150°C and 1100°C and an the exhaustive study of the peaks at 40° and 46°. The Miller Index is the same for the three temperatures.

The intensity of the peaks is directly related to the crystallinity of the phase, the most crystalline a phase is the most intense the peaks will be. By that reason it can be said that BNT-BT formed using 20% of Sodium excess is less crystalline than the obtained using a 5% excess.

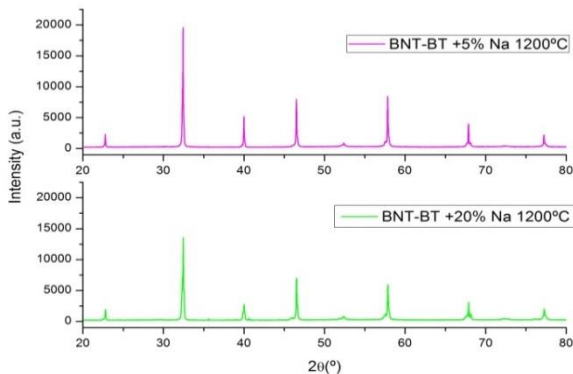


Figure 20: Comparison between XRD patterns of the BNT-BT pellets with 5% and 20% excess of Sodium.

A detailed study of the pattern revealed that near 40° there are two peaks that can't be indexed as a triclinic phase. Those peaks were also not found when treated the powder at 700°C (like the secondary phase of the 5% Sodium excess BNT-BT) and have a very low relative intensity (<1%) but can explain the existence of an unknown secondary phase rich in Na-Ti-O that was seen by the SEM-EDS characterization. This unknown secondary phase was also not observed on 5% Sodium excess pellets.

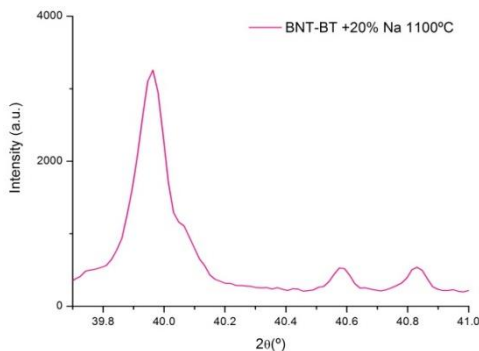


Figure 21: XRD pattern of BNT-BT with 20% Sodium excess sintered at 1100°C. The secondary phase can be seen in the form of two little peaks at 40.56° and 40.83°.

XRD patterns were analyzed with AFFMA, a program used to assign Miller Index and to determine the cell parameters using as reference XRD patterns of cubic and triclinic BNT-BT (PDF#01-089-3109 for the cubic and PDF#01-085-0530 for the triclinic). The cell parameters of each BNT-BT treatments can be found at **Table 7** where a , b and c are the length of the sides of the cell, α , β , γ are the angles and V is the volume of the cell. Density and relative density was calculated with **Equation 7** where P_M is the molecular weigh of the compound; Z is the number of unit cells, V the volume of the cell and N_A the Avogadro number.

$$\text{Equation 7: } \rho = \frac{P_M \cdot Z}{V \cdot N_A}$$

Entry	a [Å]	b [Å]	c [Å]	A[°]	B[°]	Γ[°]	V [g/cm ³]	ρ [g/cm ³]
1200°C +5%Na	5.505(1)	5.493(2)	6.7860(9)	89.86(2)	98.87(1)	120.00(2)	177.75	6.00
1150°C +5%Na	3.901(4)	3.901(4)	3.901(4)	90	90	90	59.38	5.96
1100°C +5%Na	3.9031(9)	3.9031(9)	3.9031(9)	90	90	90	59.46	5.95
1200°C +20%Na	5.497(1)	5.488(2)	6.78181	90.00(2)	89.67(2)	119.9(2)	177.34	6.02
1150°C +20%Na	5.510(1)	5.493(2)	6.7863(9)	89.83(2)	89.87(1)	120.05(9)	177.82	6.00
1100°C +20%Na	5.505(1)	5.492(2)	6.7862(9)	89.86(2)	89.87(1)	119.99(2)	177.71	6.00

Table 7: Perovskite cell parameters and density of BNT-BT with 5% and 20% Sodium excess sintered at different temperatures.

Using XRD analysis, some of the effects of the Sodium excess on BNT-BT preparation can be demonstrated. The amount of Sodium affects the perovskite structure making it more asymmetrical the most Sodium it is added and also it lowers the crystallinity of the phase obtained. In addition, the quantity of Sodium can change the secondary phase obtained as it goes from a Na_2TiO_3 secondary phase, when sintered with a 5% Sodium excess, to an unknown phase rich in Na-Ti-O when sintered with a 20% of excess.

7.4 IMPEDANCE SPECTROSCOPY (IS)

Impedance Spectrometry was used to study the effects of Sodium excess on the electrical properties of BNT-BT ceramics.

The densest pellet of each treatment was covered with a thin film of gold through a sputtering PDV. With this film both faces of the pellet act as a pair of electrodes. Once the borders have been sanded down, when a voltage is applied to the system it becomes a capacitor.

The permittivity measurements of the material were done from room temperature to 500°C. On the other hand, the permittivity was measured at different frequencies between 0.1kHz throughout the temperature range. Also, the effects of the frequency on the permittivity at room temperature were studied for frequency ranges between 0.005 kHz to 13000 kHz.

On **Figure 22.a)** it can be seen how the value of the permittivity is almost unaffected by the sintering temperature but it affects the antiferroelectric - paraelectric phase transition near 300°C. This temperature is related to the Curie temperature (T_c), which is the temperature

above which a ferroelectric substance loses its ferroelectric behavior and becomes paraelectric. The dielectric losses are low for all the ceramics studied and constantly increase with the temperature until reaching the 300°C where the three pellets have a high increment of dielectric losses, meaning the material is becoming more conductive.

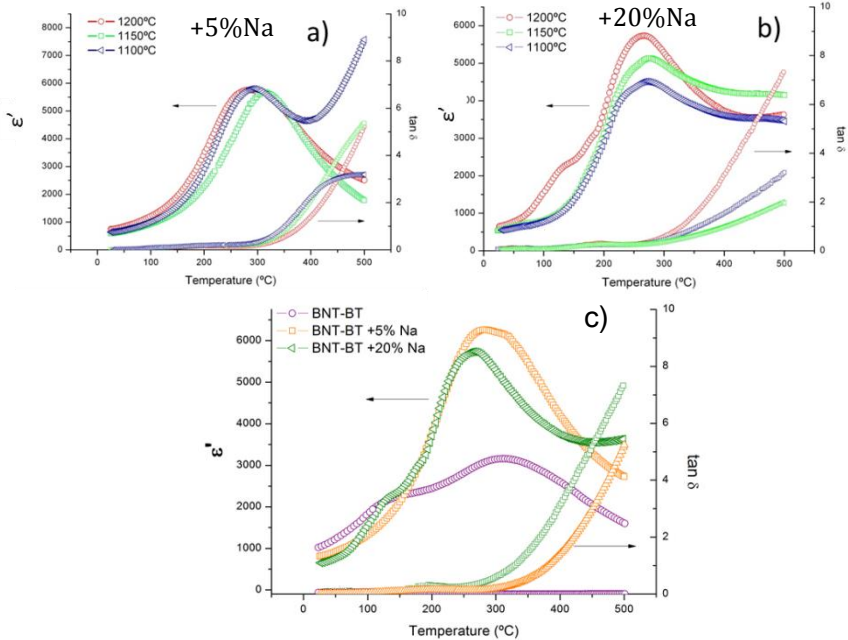


Figure 22: Permittivity (ϵ') and dielectric losses ($\tan \delta$) vs temperature at a frequency of 100 kHz for BNT-BT pellets **a)** With 5% Sodium excess **b)** 20% Sodium excess and **c)** comparison with BNT-BT without Sodium excess sintered at 1200°C.

Figure 22.b shows how a greater excess of Sodium affects the permittivity diminishing its value at each treatment. The pellet sintered at 1200°C shows two maximums meaning it had two phase transitions. The first one, around 150°C, corresponds to the ferroelectric – antiferroelectric phase transition and the second one to the antiferroelectric – paraelectric phase transition. The dielectric losses of the 20% Sodium excess pellets have higher values than the ones from 5% excess which means that the most Sodium the pellets have the less dielectric they are with the increment of temperature.

Figure 22.c is a comparison between 3 pellets with different Sodium composition sintered at 1200°C. The purple plot belongs to the BNT-BT pellet without Sodium excess. Both phase

transitions can be seen but the most valuable information this comparison gives is the permittivity value. BNT-BT pellets with 5% and 20% Sodium excess have higher permittivity values meaning the excess of Sodium allows the obtaining of new materials with higher permittivity values around the temperature of the phase transition. Also, the dielectric losses of the BNT-BT without Sodium excess are almost non-existent in the temperature range while both pellets with excess have a huge increase of the losses after the phase transition around 300°C .

Figure 23 shows the evolution of the permittivity with the frequency at room temperature. For both Sodium excess pellets, a greater sintering temperature meant greater frequency. Also it can be seen how the permittivity have higher values for the pellets with less Sodium excess.

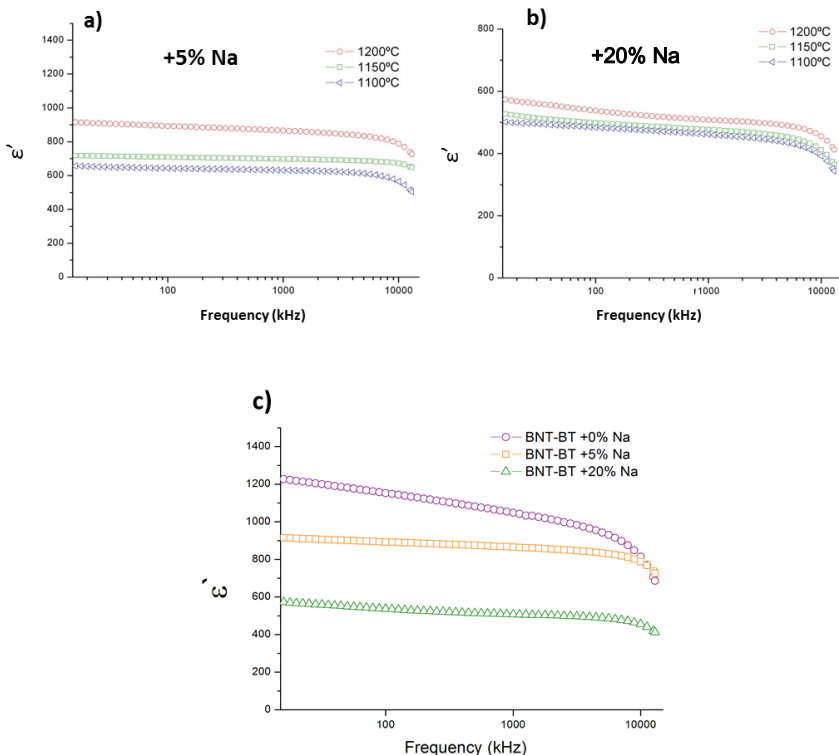


Figure 23: Permittivity vs frequency at room temperature for BNT-BT pellets with a) 5% Sodium excess b) 20% Sodium excess and c) Permittivity vs frequency at room temperature for BNT-BT pellets sintered at 1200°C

8. CONCLUSIONS

After this work has been completed, the following conclusions have been extracted:

- The ceramic method is a simple method for producing dense ceramics. The weighting of the reactants is one of the steps where it is required to work with more accuracy.
- Usual and used techniques in solid state chemistry are very useful. X-Ray Diffraction (XRD) has been proved to be a vital technique for characterization as it is a non-destructive test that shows whether there is a single-phase product or not and; once a single phase is obtained, XRD allows the determination of the crystalline structure of the product. Infrared Spectroscopy was used to analyze the bonds present in the sample, before and after calcination, in order to insure the optimization of the method.
- After the characterization of the synthesized ceramics, some conclusions were extracted:
 - a. Concerning the structure of the materials (XRD), the amount of Sodium on the structure was proved to change the degree of crystallinity and the structure of the BNT-BT. On the other hand, the most Sodium excess the less crystallinity was observed. BNT-BT with 5% Sodium sintered at 1150°C and 1100°C had pseudo-cubic structure while, at the same sintering temperatures, BNT-BT with 20% Sodium excess presented a triclinic structure. Sintering temperature affects the structure too as BNT-BT with 5% Sodium presents a triclinic structure.
 - b. Dense ceramics have been obtained with different morphology based on the Sodium excess. BNT-BT with Sodium excess present two different phases over the surface of the ceramic. The most Sodium the surface has the less homogeneous it is. Also on both compositions a Sodium Titanate phase was found. Both excesses of 5% and 20% of Sodium were proved to be ineffective at making up for the volatilization of Sodium during the sintering process as the sintered pellets had the same Sodium value as the BNT-BT without excess. Also, a Sodium Titanate phase,

not present on BNT-BT pellets without Sodium excess, was found on all the pellets with Sodium excess.

- The study of the electrical properties (IS) reflects that the ceramics with excess of Sodium present similar dielectric anomalies to BNT-BT, fact that confirmed again its obtention, but with some modifications that can be related to the effects caused by the excess of Sodium. The pellets with 5% Sodium excess have higher permittivity than ceramics with 20% Sodium excess or without any excess so it can be concluded that a soft excess of Sodium can increase the permittivity of the ceramic around the temperature of the ferroelectric–paraelectric phase transition. At the same time, the excess of Sodium results in the increasing of the dielectric losses at temperatures higher than the phase transition, therefore the new obtained ceramics present some conductivity at high temperature.

9. REFERENCES AND NOTES

1. J. Curie and P. Curie "Développement, par pression, de l'électricité polaire dans les cristaux hémihédres à faces inclinées" C. R. Acad. Sci., Paris, 91, 294 (1880).
2. Roozbeh Arshadi and Richard S. C. Cobbold. A pioneer in the development of modern ultrasound: Robert William Boyle (1883-1955). *Ultrasound in Medicine and Biology*, 33(1):3, (2007).
3. B. Jaffe, R. S. Roth, and S. Marzullo. Piezoelectric properties of lead zirconate-lead titanate solid-solutions ceramics. *Journal of Applied Physics*, 25(6):809, (1954).
4. M. Trainer "Kelvin and piezoelectricity" *Eur. J. Phys.*, vol.24 535 (2003).
5. B. Jaffe, W. R. Cook, and H. Jaffe. *Piezoelectric Ceramics*. Academic Press, USA (1971).
6. RISKIM Version 4.0. Base de datos de sustancias con clasificación y etiquetado armonizado en la Unión Europea del anexo VI del Reglamento (CE) N° 1272/2008 <http://riskim.insht.es:86/riskim/CLP/default.asp> Visited: 25-09-2015
7. EU-Directive 2002/95/EC : Restriction of the use of certain hazardous substances in electrical and electronic equipment (RoHS). *Off. J. Eur. Union*, 46, (L37), 19-23. (2003)
8. EU-Directive 2002/95/EC: Waste electrical and electronic equipment (WEEE). *Off. J. Eur. Union*, 46, (L37), 24-28 (2003)
9. T. Takenaka and Y. Masuda. *Ferroelectrics*, Vol.7 374 (1974).
10. B. Parija, T. Badapanda, S. Panigrahi, T. P. Sinha. Ferroelectric and piezoelectric properties (1-x)(Bi_{0.5}Na_{0.5})TiO₃-xBaTiO₃. *J. Mater Sci: Mater Electron*. 24:402-410 (2013).
11. T. Takenaka, K. Maruyama, K. Sakata. (Bi_{1/2}Na_{1/2})TiO₃-xBaTiO₃ System for Lead-Free Piezoelectric Ceramics. *Japanese Journal of Applied Physics*, 30(9B):2236-2239, (1991)
12. Roger H. Mitchell. *Perovskites: Modern and Ancient*. Almaz, (2002).
13. West, A. R. *Solid state chemistry and its applications*. John Wiley & sons. (1984).
14. Glazer A. M. The classification of tilted octahedral in perovskites. *Acta Crystallographica Section A*, 28(11):3384, (1979).
15. Gazer A. M. Simple ways of determining perovskite structures. *Acta Crystallographica Section A*, 31(6):756, (1975).
16. Yuan Y., Shang S., Zhou X., Liu J. Phase transition and temperature dependences of electrical properties of [Bi(Na_{1-x}K_xLi)_{0.5}]TiO₃ ceramics. *Jpn. J. Appl. Phys.*, 45:831-834. (2006).
17. Schofield D., Brown R. F. An investigation of some barium titanate compositions for transducer application. *Can. J. Phys.*, 35:594-607. (1957).
18. Ringgaard E., Wurtzlitzer T., Lead-Free piezoceramics based on alkali niobates. *J. Eur. Ceram Soc.*, 45(5):209-213. (1962).
19. Guo Y., Kakimoto K., Ohsato H. Phase transitional behavior and piezoelectric properties of (Na_{0.5}K_{0.5})NbO₃LiNbO₃ ceramics. *Appl. Phys. Lett.*, 85:4121-4123. (2004).
20. T. Rojac, M. Kosec, P. Segedin, B. Malic, and J. Holc. The formation of a carbonate complex during the mechanochemical treatment of a Na₂CO₃-Bb₂O₅ mixture. *Solid State Ionics*, 177(33-34):2987, (2006)
21. Pavan K. Heda, David Dollimore, Kenneth S. Alexander, Dun Chen, Emmeline Law, and Paul Bicknell. A method of assessing solid state reactivity illustrated by thermal decomposition experiments on Sodium bicarbonate. *Thermochimica Acta*, 255(0)_255, (1995).
22. Wang Yongli, Damajonovic Dragan, Klein Naama, and Setter Nava. High temperature instability of Li- and Ta-modified (K,Na)NbO₃ piezoceramics. *Journal of the American Ceramic Society*, 45(5):209, (1962).

